

Screening of the Anticancer Potential of Lycopene-Loaded Nanoliposomes

Ashu Saini¹, Lokvendra Singh Budania², Anupam Berwal³, Sushila Kaura⁴, Neeraj Sethi^{5*},

¹Department of Biochemistry, Om Sterling Global University, Hisar

²Department of Anesthesiology, Kalpana Chawla Government Medical College and Hospital, Karnal

³Department of Microbiology, Kalpana Chawla Government Medical College and Hospital, Karnal

⁴Department of Pharmacology, Om Sterling Global University, Hisar

⁵Department of Biotechnology, Om Sterling Global University, Hisar

Abstract

Lycopene, a naturally occurring triterpene, demonstrates significant anti-cancer potential. However, due to its limited bioavailability, it exhibits a diminished solubility in an aqueous environment. A promising technique for enhancing the solubility and bioavailability of Lycopene is the utilization of liposomal nano formulation. The present investigation involved the development of Lycopene nanoliposomes, followed by a comprehensive analysis and modification of their physical and chemical properties. Lycopene nanoliposomes exhibited favorable attributes for their prospective application in drug administration, as evidenced by their particle size distribution spanning 40-150 nm, zeta potential of -21.5mV, and an entrapment efficacy of 60.0%. The cytotoxic efficacy of a liposomal nano formulation loaded with Lycopene was established in inhibiting cancer cell proliferation, as evidenced by its impact on the A-549, MCF-7, and Hela cell lines. Consequently, the present study endeavor demonstrated the potential utility of Lycopene nanoliposomes as a viable nano formulation for the treatment of cancer.

Keywords: Nanoliposomes, Lycopene, Liposomal Nanoformulation, Cancer therapy.

Introduction

Chemotherapy works best when drugs reach their molecular targets. Anticancer drug circulation in the body is random and non-targeted, reducing its efficacy. It also raises toxicity and negative effects. Site-specific drug administration and reduced side effects are achieved by entrapping an anticancer agent in a carrier. For carrier-mediated cancer medicine delivery, the particle's surface must have a suitable agent and be biocompatible [1].

Nanotechnology could improve cancer diagnosis and treatment [2]. Many nanotechnologies have been created to treat cancer more efficiently and safely due to the disadvantages of standard chemotherapy. Over 40 nanotherapeutics, including chemotherapeutics and imaging agents, have been given to patients. A nanomaterial platform can integrate many therapeutic effects [3]. For this reason, they can target specific tissues. Effective systemic distribution of nanotherapeutics to solid tumors requires a better understanding of their biological and physicochemical properties [4].

Non-immunogenic, biocompatible, and degradable nanoliposomes are widely used drug delivery [5]. Additionally, liposomal bioactive administration increases bioactive ingredient bioavailability as it passes through the digestive tract and into the bloodstream. Hydrophilic components dissolve into nanoliposomes' watery centers during formulation, while hydrophobic materials bond to the bilayer. Nanoliposomes can use hydrophilic and hydrophobic bioactive substances. Since phyto nanoformulations were discovered and refined, advanced nano-herbal products can be made [6]. Many herbal medications address CVS, respiratory, diabetes, cancer, and other conditions.

Nanoformulations have improved cancer treatment, reducing disease severity and death. Lycopene possesses anti-inflammatory and hepatoprotective properties [7, 8]. Lycopene triterpenoids include free carboxylic acid and saponin aglycone [8]. It alters the glucocorticoid receptor and reduces Bcl2 in Michigan Cancer Foundation-7 breast cancer cell lines [9, 10]. Due to its low toxicity and natural origin, lycopene is used in pharmaceutical formulations for local and oral use [11, 12]. The Lycopene-loaded novel liposomal nano formulation may overcome such constraints and distribute Lycopene. Lycopene nanoliposomes may increase solubility, bioavailability, and therapeutic potential. Lycopene nanoliposomes were developed, characterized, and tested for anti-cancer efficacy against cancer cell lines.

Materials and methods

Drug and chemicals

Lycopene came from India, from a company called Sigma Aldrich. Cholesterol came from a place called Molychem in Mumbai. Cell lines A-549 (Human lung adenocarcinoma epithelial cells), MCF-7 (Human breast adenocarcinoma cells), and Hela (Human cervical carcinoma cell line) were obtained from the National Center for Cell Science (NCCS), Pune; whereas, Lecithin, Minimum Essential Eagle Medium, Foetal Bovine Serum (FBS), penicillin, and streptomycin were purchased from Himedia, Mumbai. All of the substances used in the experiments were of analytical reagent quality.

Preparation of Lycopene nanoliposomes

Lycopene nanoliposomes (LNLs) were made by thin film hydration. Both lecithin and cholesterol were utilized as excipients. 28 milliliters of ethanol and 70

milliliters of carbon tetra chloride were combined with 650 milligrams of lecithin, 100 milligrams of cholesterol, 20 milligrams of cetyl trimethyl ammonium chloride, and 200 milligrams of lycopene. For 4.5 hours at 42 degrees, the mixture was evaporated in a rotary evaporator to create a lipid film. The film was then hydrated in 90 ml of deionized water containing 2 ml of 0.035% Tween-80 solution at 70 degrees Celsius for an hour. The large, stable, and well-hydrated multilamellar vesicle suspension that resulted was then subjected to sonication and extrusion.

Characterization of Lycopene nanoliposomes

Dynamic light scattering was used to determine the average nanoliposome particle size and the degree of heterogeneity (polydispersity index) of size-optimized nanoliposomes. The Zetasizer Nano ZS-90 (Malvern Instruments, Malvern, UK) was used to assess the electrokinetic potential in a colloidal dispersion of vesicles, which indicated whether or not the liposomal nanoformulations were stable at 25 °C. The amount of unbound medication in the supernatant was measured after centrifugation at 10,000 rpm, 4 °C for 30 min, and the % encapsulation efficiency was computed. A transmission electron microscope (TEM-Hitachi-H-7501SSP/N-817-0520, Japan) was used to examine the better batch for morphological defects. One drop of optimized LNLs was placed on a copper grid, air-dried, and scanned at 60,000x magnification and 80,000 V accelerating voltage to create a TEM micrograph. Before LNLs were extruded, their morphology was analyzed under a fluorescent photomicroscope (LEICA DM 2500 M) at 100X magnification. The KBr pellet of powdered samples of Lycopene, lecithin, cholesterol, and LNLs was analyzed in the range of 4500-500 cm⁻¹ using the FTIR spectrophotometer Affinity-1 (Shimadzu, Japan). The physical properties of the drug and liposomes were determined by performing a differential scanning calorimetry-thermogravimetric analysis (DSC-TGA) on LNLs and dummy nanoparticles using a TGA/DSC 3+ Stare System, Mettler Toledo AG, Analytical, Switzerland. Samples (5 mg) were scanned between 30 and 500 C using an alumina pan and a heat flow rate of 15 C/min.

In vitro release profile of Lycopene nanoliposomes

The release profile was studied using the dialysis sac technique. Dialysis sacs containing 10 mg of LNLs were immersed in a solution of 25% ethanol and 0.1 M phosphate buffer saline at a pH of 7.4, and the mixture was then stirred continuously at 90 rpm at a temperature of 37 °C. There were 24 total samples taken, each

measuring 1 ml in volume, taken at 1, 2, 3, 6, and 24-hour intervals. The samples were then analyzed by high-performance liquid chromatography (Agilent 1200 Infinity Series) at 216 nm for 8.24 min using a ZORBAX SBC-18 column that was five meters long and had a particle size of 4.6 microns by 4.6 micrometers.

Antioxidant activity

Antioxidant activity was determined as a measure of antioxidants' capacity to quench DPPH. Lycopene and LNLs were treated with 1, 1-diphenyl-2-picrylhydrazyl (DPPH), a free radical solution in methanol (3.9 mg/100 ml), for 30 minutes at room temperature in the dark. Absorption was measured using a UV spectrophotometer at 517 nm. Nanoliposomes devoid of lycopene, as a positive control, and lycopene, as a negative control, as well as LNLs, were tested for their ability to inhibit DPPH. Using the equation provided below, we were able to determine the relative DPPH inhibition of pure Lycopene and lycopene-loaded nanoliposomes.

$$\text{Percent antioxidant activity} = \frac{(\text{Control Abs.}) - (\text{Sample Abs.})}{(\text{Control Abs.})} \times 100$$

In-vitro cytotoxic assay

LNLs solutions' in vitro cytotoxicity was evaluated using the MTT assay on A-549 (human lung adenocarcinoma epithelial cells), MCF-7 (human breast adenocarcinoma cells), and Hela (human cervical carcinoma cell line). Tetrazolium dye assays are used to determine the cytotoxic or cytostatic effects of a therapeutic bioactive agent or potentially dangerous chemicals. Experiments using MTT reagent are normally conducted in a dark atmosphere [11] because to the reagent's sensitivity to light. Both normal and malignant cell lines were cultured in a humidified incubator at 37 degrees Celsius and 5% carbon dioxide using a medium containing 10% inactivated fetal bovine serum, 100 units per milliliter of streptomycin, and 100 units per milliliter of penicillin. After the cells reached 70% confluence, they were subcultured in a 0.25% trypsin solution in a sterile environment. Dilutions of 1 M, 10 M, 20 M, 50 m, and 100 m per ml were produced in the medium on 96-well plates using DMSO (M/ml) stock solutions of the compound and the standard. The proliferation characteristics of each cell line were used to determine their respective densities. After an initial incubation period of 8 hours, duplicate wells were treated with varying concentrations of LNL (0.1-1000 g/ml) and Lycopene for an additional 3 days. After three days, 3 liters (5 mg/ml) of MTT solution were added to the growth media. The results were based on the mitochondrial conversion of 3-(4,5-dimethylthiazol-2-yl) 2,5-diphenyltetrazolium bromide (MTT) over a period of 180 minutes of incubation. All of the metabolically active cell percentage was compared to Formazan crystals and untreated controls. After dissolving formazan crystals in DMSO, the absorbance at 570 nm was measured using a microplate reader (BIORAD). The effectiveness of synthetic chemicals against cancer was measured in comparison to Lycopene.

Results and Discussion

Synthesis of Lycopene Nanoliposomes (LNLs)

Thin-film hydration was used in the production of Lycopene nanoliposomes. Since nanoliposomes have both lipid and aqueous phases, they can be employed for the capture, transport, and release of both lipid- and water- soluble compounds. In the present study, Lycopene, a hydrophobic drug, showed an overall improvement in its pharmacological profile after being absorbed into the liposomes.

Characterization of Lycopene Nanoliposomes

Particle size analysis and Zeta potential

Particle size matters for liposomal nanocarriers. Cellular absorption, drug release, encapsulation, and bio-distribution are affected [12,13]. A 150-nm nanoliposome can enter or leave cancer cells' microenvironment. Malignant cells are bigger and vascular [14]. Tumor locations will accumulate vascular mediators. However, cancer cells' permeable vasculature allows high molecular weight medicines to boost EPR. Drugs in 400-nm liposomes passively target cancer cells but are blocked from healthy tissues by the endothelium [15–20]. The current investigation found 211 nm LNL particles, indicating significant vasculature and accumulation. Zeta potential calculations assessed surface charge and stability [21–22]. Zeta potential regulates nano liposomal fusion, precipitation, and aggregation. A higher negative value indicates increased stability and cellular absorption. The zeta potential of LNLs was -42.5 mV, indicating better stability.

Percent encapsulation efficiency (% EE)

LNLs formulation encapsulation efficacy was determined from dispersion medium free drug concentration. HPLC was used to compute free Lycopene in the supernatant after centrifuging for 30 min at 10,000 rpm (4 C) (Fig. 1). The following equation calculates encapsulation efficiency.

$EE(\%) = \{(C_{\text{initial}} - C_{\text{final}})/C_{\text{initial}}\} \times 100$ Where, C_{initial} - initial drug concentration and the C_{final} - free drug measured in the supernatant after centrifugation. The percent encapsulation was found to be 65.2% for Lycopene.

Morphological studies using Photomicroscopy and TEM

LNLs formulation encapsulation efficacy was determined from dispersion medium free drug concentration. HPLC was used to compute free Lycopene in the supernatant after centrifuging for 30 min at 10,000 rpm (4 C) (Fig. 1). The following equation calculates encapsulation efficiency.

FTIR spectroscopy

Due to the intense interaction between medications and excipients, FTIR can distinguish several functional groups, provide structural information in the form of peaks or spectra, and detect molecular arrangement changes. Lycopene has a unique FTIR signal for the -OH stretch at 3447 cm⁻¹. The FTIR peak for -CH₂

group vibrations is 3030 cm⁻¹. The 1742 cm⁻¹ FTIR signal indicates the C=O functional group. Stretch-OH FTIR peak 1318 cm⁻¹. Stretch (C-O group) peaks at 1043 and 1421 cm⁻¹ (Fig. 3A). An FTIR signal for cholesterol is the hydroxyl group at 3512 cm⁻¹. Fig. 3B shows that the aromatic stretch of CH=CH, carboxylic acid C=O group, and ester stretch cause the peaks at 2930 cm⁻¹, 1565 cm⁻¹, and 988 cm⁻¹, respectively. The FTIR peak of the amide group at 3546 cm⁻¹ is lecithin's. The P-O-C stretch vibration is at 1011 cm⁻¹, the P=O stretch vibration is at 1320 cm⁻¹, and the -OH carboxylic stretch vibration is at 2989 cm⁻¹ (Fig. 3C).

LNLs' FTIR spectrum shows Lycopene, cholesterol, and lecithin peaks. The hydroxyl group peaks at 3445 cm⁻¹, the aromatic CH=CH stretch at 3023 cm⁻¹, the carboxylic acid C=O group at 1501 cm⁻¹, and the cholesterol ester stretch at 909 cm⁻¹ (Fig. 3D).

Amide has a peak at 3021 cm⁻¹, a -OH carboxylic stretch vibration at 2897 cm⁻¹, a P=O stretch vibration at 1365 cm⁻¹, and a P-O-C stretch vibration at 1102 cm⁻¹. The FTIR peaks indicate Lycopene. The -OH group (Stretch) FTIR peak is 1390 cm⁻¹, while the -CH₂ group vibrations are 3012 cm⁻¹. Stretch, or the C-O group, peaked at 965 and 1300 cm⁻¹. P=O shifts from 1338 cm⁻¹ to 1387 cm⁻¹ and P-O-C shifts from 988 cm⁻¹ to 999 cm⁻¹ when Lycopene and lecithin interact. **Differential Scanning calorimetric and Thermogravimetric analytical studies**

Two endothermic peaks appeared on the free Lycopene DSC thermogram. The low strength of the first endothermic peak at 286 oC confirmed Lycopene's presence, whereas the high intensity of the second peak revealed its crystalline shape (29–30). The thermogram for LNLs showed an endothermic peak at 375 oC and disintegration around 370 oC (Fig. 4A). The low peak intensity encouraged LNLs' amorphousness. Blank nanoliposomes showed two endothermic peaks: a low intensity peak at 170 oC and a second peak at 365 oC that decomposes beyond 365 oC (Fig. 4B). The peaks were not sharp due to its uniqueness.

To determine temperature-related weight loss, TGA was used. At 340 oC, false nanoliposomes lost the most weight, but LNLs lost the most at 350 oC following a slight melting temperature change, suggesting a co-amorphous phase difference.

In vitro drug release profile for LNLs using HPLC

Controlled medication release from the nanoparticle matrix prevents increased metabolism and degradation. In- vitro drug release data showed 85.6% pure Lycopene released in 3 hours. Only 38.9% Lycopene was released from LNLs after 3 hours of steady release. 71.6% of Lycopene was LNL-free in 24 hours. LNL drug release profiles show continuous Lycopene release because Lycopene is hydrophobic (nonpolar). Liposomal nanoformulations formed thick, firmly walled lipid bilayers around Lycopene particles to prolong release

(Fig. 5).

Antioxidant activity

DPPH assay is commonly used to assess encapsulated compound antioxidant activity [31, 32]. The stable free radical 1,1-diphenyl-2-picrylhydrazyl is rich violet because it has spare electrons throughout the molecule. The absorption band is 517 nm [33-34]. Violet colour fades when DPPH is uniformly mixed with an oxidising hydrogen molecule. The antioxidant Lycopene is frequently utilized. Adding DPPH (a hydrogen atom donor) to Lycopene solution turned it violet to pale yellow. Thus, the absorption band shrank. LNLs inhibited DPPH better than free Lycopene. Nanoencapsulating Lycopene by lipid bilayer reduces its nanoscale size and exposes more surface, increasing antioxidant action (Fig. 6).

Anticancer activity

A-549, MCF-7, and HeLa cell lines were used to investigate Lycopene and LNLs for anticancer activities using the MTT assay. The results are in Table 1. LNLs are harmful because nanoliposomes have a large surface area. Deeper tumor penetration is better with smaller bilayer vesicles [35–37]. The literature reports Lycopene's anti-cancerous capabilities [38]. Healthy cells contain mitochondrial dehydrogenase. It breaks down the pale yellow MTT dye's tetrazolium ring structure [39] to make dark purple formazan crystals that

accumulate up inside cells [40–45]. Lycopene isomer oleanolic acid in a liposomal nanopatforms caused apoptosis and cytotoxicity in cancer cells. In general, mPEG-PLA/PLGA-loaded NPs were more cytotoxic to cancer cells and delivered oleanolic acid better [43]. LNLs showed significant anticancer effects against A-549, MCF-7, and HeLa celllines with IC50 values of 5.8 g/ml, 5.2 g/ml, and 4.9 g/ml, respectively. This effect was stronger than that of pure BA particles, which exhibited IC50 values of 26.66, 25.89, and 31.

Conclusions

Phytochemicals have been employed for many therapeutic purposes due to their beneficial benefits and low toxicity. This study described LNL preparation, characterization, optimization, and in vitro antioxidant and anticancer characteristics. Lycopene's size was lowered by lipid bilayer vesicles, increasing bioavailability and release. Lipid-based nanoformulations provide low-dose Lycopene therapy and better medication residence time. Nanoliposomes (lipid bilayers) can distribute bioactive compounds straight into cells and are plasma membrane-compatible. We found that LNLs were more effective in fighting cancer in vitro than structural counterparts. This makes LNLs potentially effective in cancer treatment.

Conflict of Interest

There is no conflict of interest whatever.

- #### References
- [1] Peer, D., & Margalit, R. (2004). Tumor-targeted hyaluronan nanoliposomes increase the antitumor activity of liposomal doxorubicin in syngeneic and human xenograft mouse tumor models. *Neoplasia* (New York, NY), 6(4), 343.
 - [2] Preiss, M. R., & Bothun, G. D. (2011). Stimuli-responsive liposome-nanoparticle assemblies. *Expert opinion on drug delivery*, 8(8), 1025-1040..
 - [3] Schroeder, A., Heller, D. A., Winslow, M. M., Dahlman, J. E., Pratt, G. W., Langer, R., & Anderson, D. G. (2012). Treating metastatic cancer with nanotechnology. *Nature Reviews Cancer*, 12(1), 39.
 - [4] Shi, J., Kantoff, P. W., Wooster, R., & Farokhzad, O. C. (2017). Cancer nanomedicine: progress, challenges and opportunities. *Nature Reviews Cancer*, 17(1), 20.
 - [5] Zamboni, W. C. (2005). Liposomal, nanoparticle, and conjugated formulations of anticancer agents. *Clinical cancer research*, 11(23), 8230-8234.
 - [6] Allen, T. M., & Cullis, P. R. (2013). Liposomal drug delivery systems: from concept to clinical applications. *Advanced drug delivery reviews*, 65(1), 36-48.
 - [7] de los Reyes, C., Zbakh, H., Motilva, V., & Zubía, E. (2013). Antioxidant and anti-inflammatory meroterpenoids from the brown alga *Cystoseira usneoides*. *Journal of natural products*, 76(4), 621-629.
 - [8] Yogeewari, P., & Sriram, D. (2005). Sethi, N., Bhardwaj, P., Kumar, S., & Dilbaghi, N. (2019). Development and Evaluation of Ursolic Acid Co-Delivered Tamoxifen Loaded Damar Gum Nanoparticles to Combat Cancer. *Advanced Science, Engineering and Medicine*, 11(11), 1115-1124.
 - [9] Sethi, N., Bhardwaj, P., Kumar, S., & Dilbaghi, N. (2019). Development And Evaluation Of Ursolic Acid Loaded Eudragit-E Nanocarrier For Cancer Therapy. *International Journal of Pharmaceutical Research* (09752366), 11(2)..
 - [10] Saneja, A., Kumar, R., Singh, A., Dubey, R. D., Mintoo, M. J., Singh, G., ... & Gupta, P. N. (2017). Development and evaluation of long-circulating nanoparticles loaded with betulinic acid for improved anti-tumor efficacy. *International journal of pharmaceuticals*, 531(1), 153-166.
 - [11] Vivek, V., Sethi, N., & Kaura, S. (2022). Green synthesis and evaluation of antibacterial activity of zinc nanoparticles from *Calotropis procera* leaves..
 - [12] Danaei, M., Dehghankhold, M., Ataei, S., Hasanzadeh Davarani, F., Javanmard, R., Dokhani, A., & Mozafari, M. (2018). Impact of particle size and polydispersity index on the clinical applications of lipidic nanocarrier systems. *Pharmaceutics*, 10(2), 57.
 - [13] Blasi, P., Giovagnoli, S., Schoubben, A., Ricci, M., & Rossi, C. (2007). Solid lipid nanoparticles for targeted brain drug delivery. *Advanced drug delivery reviews*, 59(6), 454-477.
 - [14] Kaura, S., Parle, M., Insa, R., Yadav, B. S., &

- Sethi, N. (2022). Neuroprotective effect of goat milk. *Small Ruminant Research*, 214, 106748..
- [15] Dhanda, P., Sura, S., Lathar, S., Shoekand, N., Partishtha, H., & Sethi, N. (2022). Traditional, phytochemical, and biological aspects of Indian spider plant..
- [16] De Leo, V., Maurelli, A. M., Giotta, L., & Catucci, L. (2022). Liposomes containing nanoparticles: preparation and applications. *Colloids and Surfaces B: Biointerfaces*, 112737.
- [17] Hussein, H. A., & Abdullah, M. A. (2022). Novel drug delivery systems based on silver nanoparticles, hyaluronic acid, lipid nanoparticles and liposomes for cancer treatment. *Applied Nanoscience*, 12(11), 3071-3096.
- [18] Poonam, D., Sethi, N., Pal, M., Kaura, S., & Parle, M. (2014). Optimization of shoot multiplication media for micro propagation of *Withaniasomnifera*: an endangered medicinal plant. *Journal of Pharmaceutical and Scientific Innovation (JPSI)*, 3(4), 340-343.
- [19] Suman, J., Neeraj, S., Rahul, J., & Sushila, K. (2014). Microbial synthesis of silver nanoparticles by *Actinotalea* sp. MTCC 10637. *American Journal of Phytomedicine and Clinical Therapeutics*, 2, 1016-23.
- [20] Milind, P., Sushila, K., & Neeraj, S. (2013). Understanding gout beyond doubt. *International Research Journal of Pharmacy*, 4(9), 25-34.
- [21] Sethi, N., Kaura, S., Dilbaghi, N., Parle, M., & Pal, M. (2014). Garlic: A pungent wonder from nature. *International research journal of pharmacy*, 5(7), 523-529.
- [22] Song, J. W., Liu, Y. S., Guo, Y. R., Zhong, W. X., Guo, Y. P., & Guo, L. (2022). Nano-liposomes double loaded with curcumin and tetrandrine: preparation, characterization, hepatotoxicity and anti-tumor effects. *International Journal of Molecular Sciences*, 23(12), 6858.
- [23] Vivek, V., Sethi, N., & Kaura, S. (2022). Green synthesis and evaluation of antibacterial activity of zinc nanoparticles from *Calotropis procera* leaves.
- [24] Sethi, N., Kaura, S., Dilbaghi, N., Parle, M., & Pal, M. (2014). Garlic: A pungent wonder from nature. *International research journal of pharmacy*, 5(7), 523-529..
- [25] Shekunov, B. Y., Chattopadhyay, P., Tong, H. H., & Chow, A. H. (2007). Particle size analysis in pharmaceuticals: principles, methods and applications. *Pharmaceutical research*, 24(2), 203-227.
- [26] Kumar, R., Sethi, N., & Kaura, S. (2022). Bio-processing and analysis of mixed fruit wine manufactured using *Aegle marmelos* and *Phoenix dactylifera*..
- [27] Aswathy, M., Vijayan, A., Daimary, U. D., Girisa, S., Radhakrishnan, K. V., & Kunnumakkara, A. B. (2022). Betulinic acid: A natural promising anticancer drug, current situation, and future perspectives. *Journal of Biochemical and Molecular Toxicology*, e23206.
- [28] Singh, A., Vengurlekar, P. R. E. R. A. N. A., & Rathod, S. (2014). Design, development and characterization of liposomal neem gel. *Int J Pharm Sci Res*, 5, 140-148.
- [29] Al-Jamal, W. T., & Kostarelos, K. (2007). Liposome-nanoparticle hybrids for multimodal diagnostic and therapeutic applications.
- [30] Albanese, A., Tang, P. S., & Chan, W. C. (2012). The effect of nanoparticle size, shape, and surface chemistry on biological systems. *Annual review of biomedical engineering*, 14, 1-16.
- [31] Kaura, S., Parle, M., Insa, R., Yadav, B. S., & Sethi, N. (2022). Neuroprotective effect of goat milk. *Small Ruminant Research*, 214, 106748..
- [32] Danaei, M., Dehghankhold, M., Ataei, S., Hasanzadeh Davarani, F., Javanmard, R., Dokhani, A., ... & Mozafari, M. (2018). Impact of particle size and polydispersity index on the clinical applications of lipidic nanocarrier systems. *Pharmaceutics*, 10(2), 57.
- [33] Geze, A., Putaux, J. L., Choisnard, L., Jehan, P., & Wouessidjewe, D. (2004). Long-term shelf stability of amphiphilic β -cyclodextrin nanosphere suspensions monitored by dynamic light scattering and cryo- transmission electron microscopy. *Journal of microencapsulation*, 21(6), 607-613.
- [34] Fontanay, S., Kedzierewicz, F., Duval, R. E., & Clarot, I. (2012). Physicochemical and thermodynamic characterization of hydroxy pentacyclic triterpenoic acid/ γ -cyclodextrin inclusion complexes. *Journal of Inclusion Phenomena and Macrocyclic Chemistry*, 73(1-4), 341-347.
- [35] Chen, X., Lu, S., Gong, F., Sui, X., Liu, T., & Wang, T. (2022). Research on the synthesis of nanoparticles of Lycopene and their targeting antitumor activity. *Journal of Biomedical Materials Research Part B: Applied Biomaterials*.
- [36] Molyneux, P. (2004). The use of the stable free radical diphenylpicrylhydrazyl (DPPH) for estimating antioxidant activity. *Songklanakarin J. Sci. Technol*, 26(2), 211-219.
- [37] Kumar, Rakesh, Neeraj Sethi, and Sushila Kaura. "Bio-processing and analysis of mixed fruit wine manufactured using *Aegle marmelos* and *Phoenix dactylifera*." (2022)..
- [38] Kong, B., Zhang, H., & Xiong, Y. L. (2010). Antioxidant activity of spice extracts in a liposome system and in cooked pork patties and the possible mode of action. *Meat science*, 85(4), 772-778.
- [39] Castan, L., del Toro, G., Fernández, A. A., González, M., Ortíz, E., & Lobo, D. (2013). Biological activity of liposomal vanillin. *Journal of medicinal food*, 16(6), 551-557.
- [40] Fujiwara, Y., Takeya, M., & Komohara, Y. (2014). A novel strategy for inducing the antitumor effects of triterpenoid compounds: blocking the protumoral functions of tumor-associated macrophages via STAT3 inhibition. *BioMed research international*, 2014.
- [41] Mosmann, T. (1983). Rapid colorimetric assay for cellular growth and survival: application to

- [42] proliferation and cytotoxicity assays. Journal of immunological methods, 65(1-2), 55-63.
- [43] de Pace, R. C. C., Liu, X., Sun, M., Nie, S., Zhang, J., Cai, Q., & Wang, S. (2013). Anticancer activities of (-)-epigallocatechin-3-gallate encapsulated nanoliposomes in MCF7 breast cancer cells. Journal of liposome research, 23(3), 187-196.
- [44] Ma, J., Guan, R., Shen, H., Lu, F., Xiao, C., Liu, M., & Kang, T. (2013). Comparison of anticancer activity between lactoferrin nanoliposome and lactoferrin in Caco-2 cells in vitro. Food and chemical toxicology, 59, 72-77.
- [45] Gerlier, D., & Thomasset, N. (1986). Use of MTT colorimetric assay to measure cell activation. Journal of immunological methods, 94(1-2), 57-63.
- [46] V. Meerloo, J., Kaspers, G. J., & Cloos, J. (2011). Cell sensitivity assays: the MTT assay. In Cancer cell culture (pp. 237-245). Humana Press.

Figure 1: Zeta potential of Lycopene loaded nanoliposomes

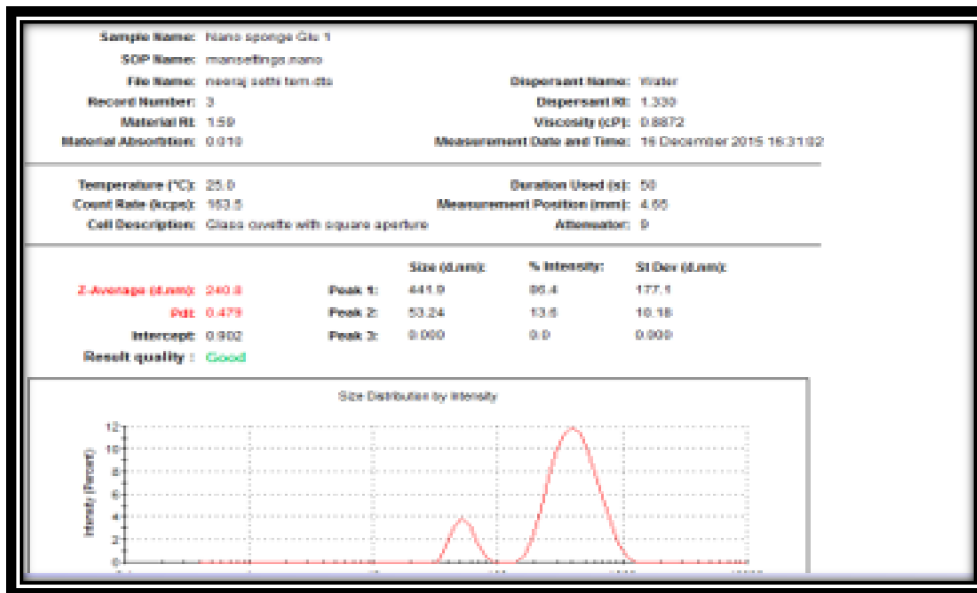


Figure 2: TEM and Photomicroscopic images of Lycopene loaded nanoliposomes

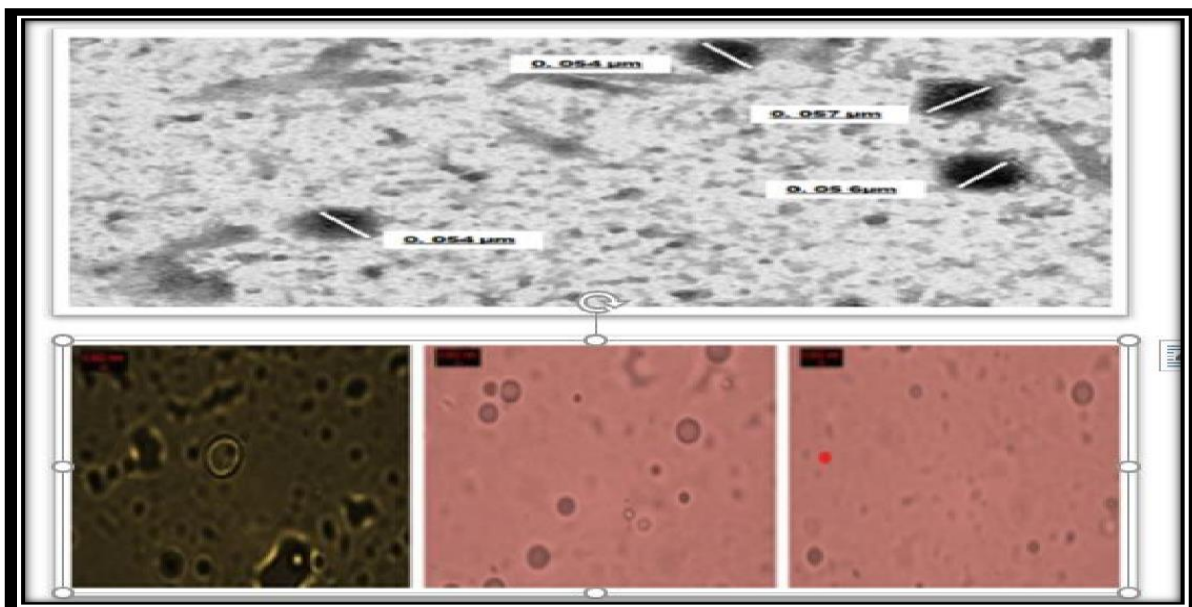


Figure 3. FTIR spectra of (A) Lycopene, (B) Cholesterol, (C) Lecithin, (D) Lycopene loaded liposomal nanoformulations

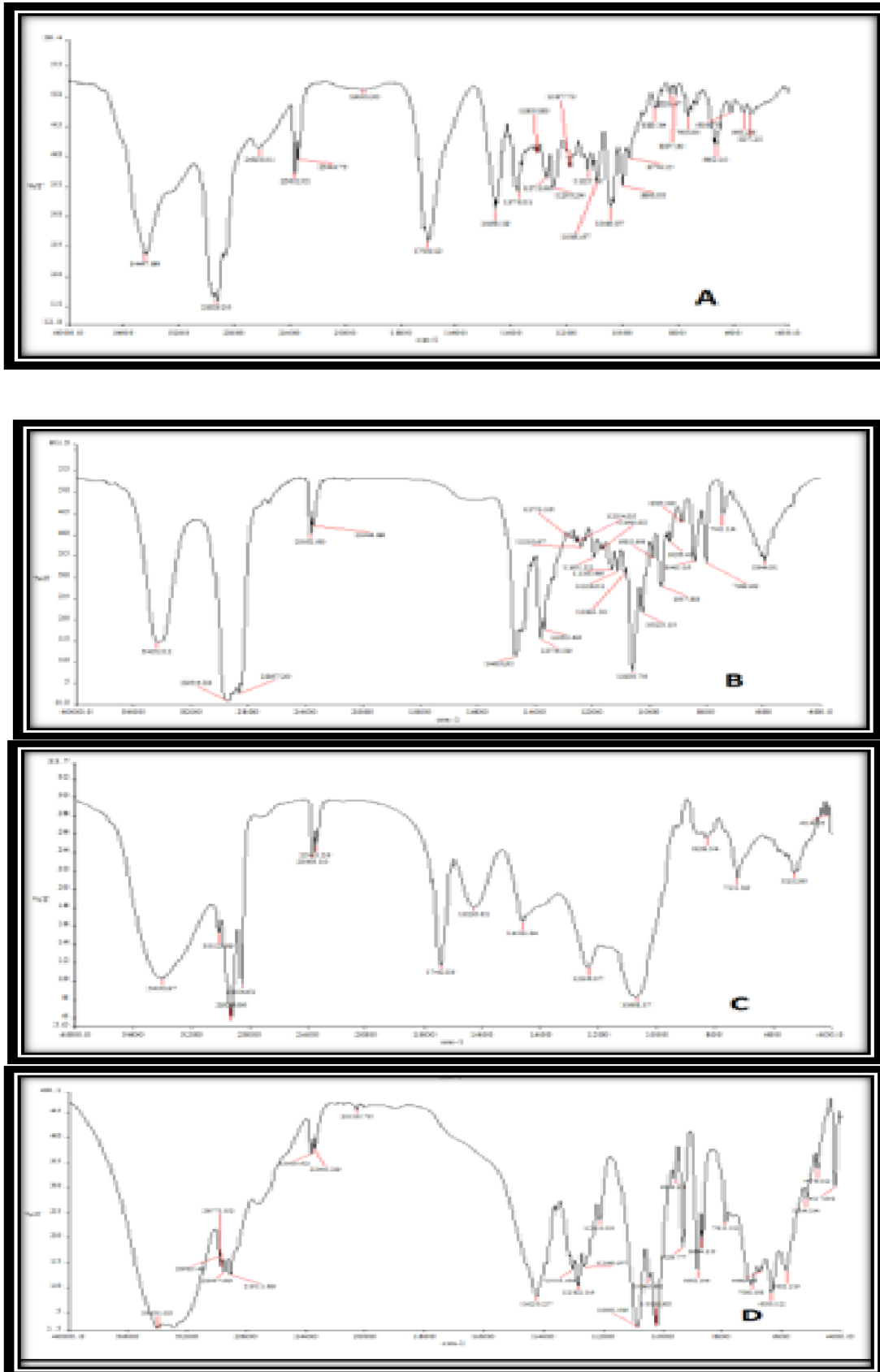


Figure 4. DSC of Lycopene loaded liposomal nanoformulations (A).

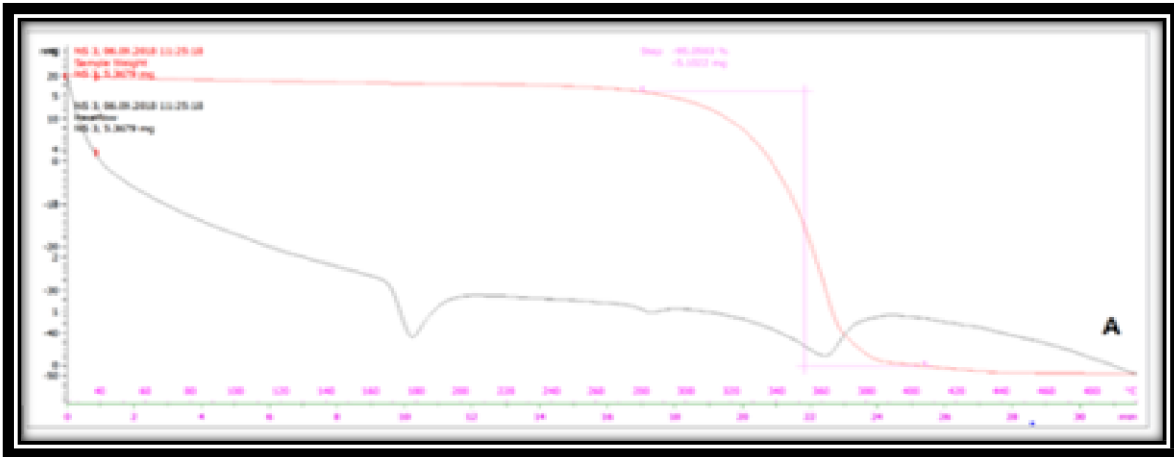


Figure 5. In vitro drug release of Lycopene nanoliposomes

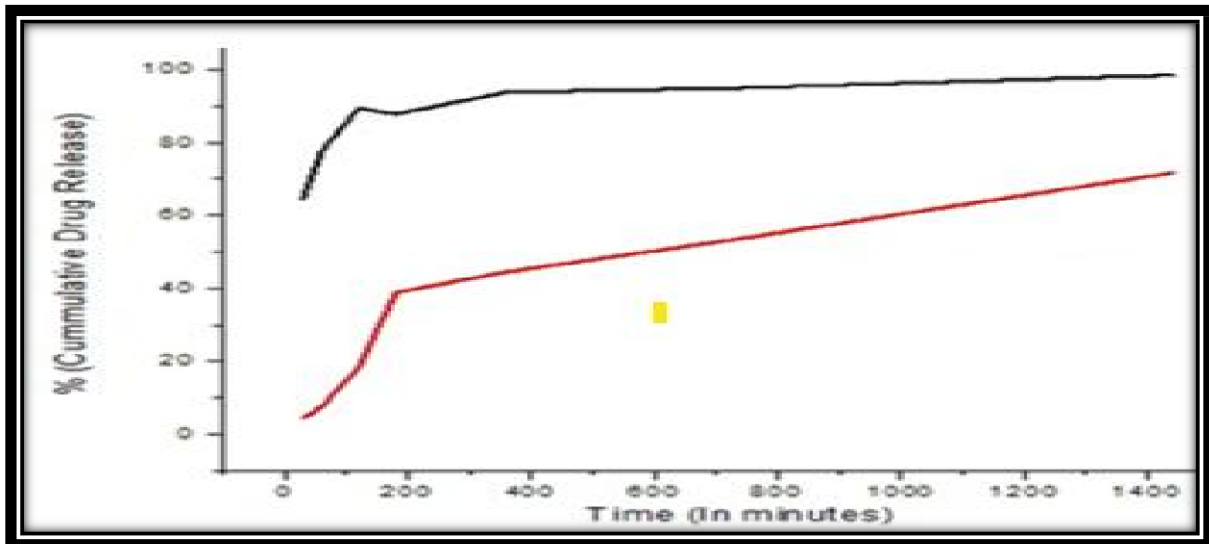


Figure 6. Antioxidant activity of Lycopene nanoliposomes

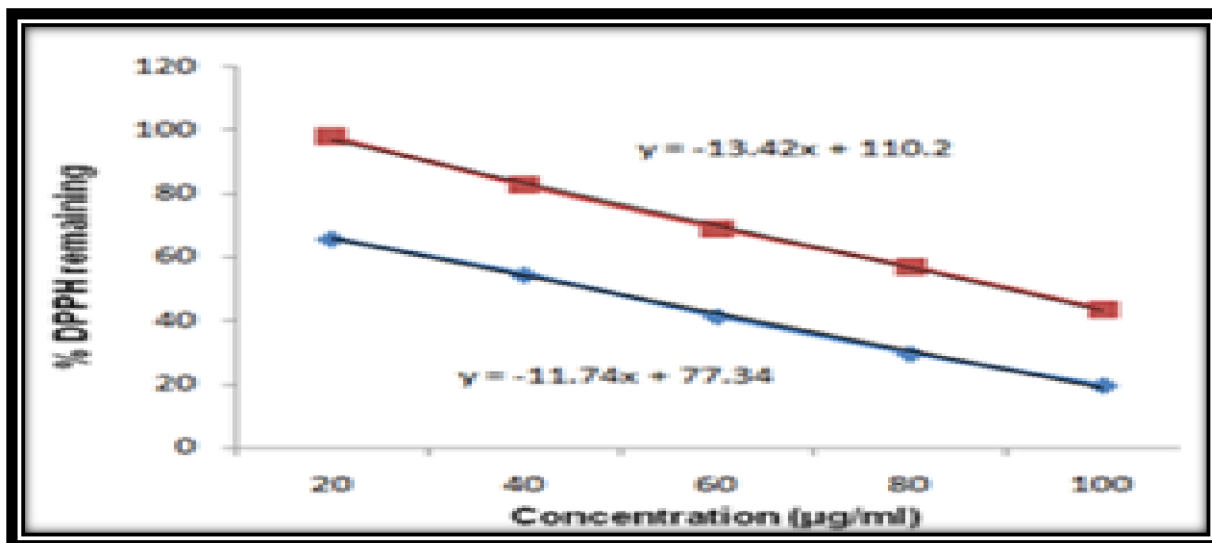


Table 1: IC50 values of LNPs along with pure drug Lycopene

Samplecode	A-549		MCF-7		Hela	
	IC50	pIC50	IC50	pIC50	IC50	pIC50
Lycopene	28.42	1.5663	26.34	-1.4913	30.98	-1.51132
LNLs	6.3	-0.84345	6.1	-0.7480	4.8	-0.6812

Figure 7. Percentage cell inhibition of LNLs on MCF-7, A-549 and MCF-7 Cell lines after 24 h.

